UNIVERSITY OF CRETE

DEPARTMENT OF MATERIALS SCIENCE AND TECHNOLOGY

BACHELOR THESIS

SYNTHESIS AND CHARACTERIZATION OF BIODEGRADABLE DIBLOCK AND TRIBLOCK COPOLYMERS FOR OCULAR DRUG DELIVERY

GEORGIOS DIMITRIOS FERGADIS

Supervisor: Prof. Maria Vamvakaki

HERAKLION 2020

Acknowledgments

This bachelor thesis is my first research work which introduced me in polymer chemistry and helped me broaden my horizon about this fascinating field. I would like thank my supervisor Professor Maria Vamvakaki who gave me the opportunity to work in her lab and guided me through the whole process and Professor Anna Mitraki for participating in my committee. Also I would like thank and express my gratitude to the postgraduate student, Ms Maria Psarrou who helped me throughout the year by giving me advices, supporting me and evaluating my progress and being patient with me. Next I would like to thank my colleagues of the Synthetic Chemistry lab for all the help and support.

I could not left out the assistance and support that I had outside the lab.A big thank you goes to my friends, especially Eirini Ailamaki and Eirini Fanouraki who understood me and who where there when I was upset and helped me overcome any problems I had. The support I had from them really helped me complete this work.

Last but not least I would like to thank my parents, Stamatis and Eleni as well as my brother Fotis for all the help and support I received all these years as, especially as an undergraduate student and for providing me with all the essentials throughout my life. I really could not thank them enough.

Contents

Abstract

Efficient drug delivery to the ocular tissues faces several challenges due to the presence of several dynamic and static barriers, such as the blood–ocular barrier, tear formation and the low permeability of the cornea. In addition, because of the very low drug bioavailability in the ocular area, repeated intraocular injections are required. Several nanomedicines have been formulated and evaluated for ocular drug delivery over the years, among which are polymeric micelles, liposomes, hydrogels, polymer-drug and protein-drug conjugates [1]. However, to the best of our knowledge, there are no examples of biodegradable systems, comprising materials which are approved by the Food and Drug Administration (FDA), being also capable of slowing down the release profile of drug, reported in the literature. Hence, the development of drug delivery systems that can ensure a suitable drug concentration for a prolonged time in different ocular tissues is certainly of great importance. In the present thesis, we aimed to develop polymeric nanocarriers for the encapsulation and delivery of Flurbiprofen, a nonsteroidal anti-inflammatory drug sold in the market in the form of a solution under the brand names Ocufen® and Ocuflur®.

In the first part of this thesis, amphiphilic poly(ethylene glycol)-*block*-poly(l-lactide) (PEG-*b*-PLLA) diblock and PLLA-*b*-PEG-*b*-PLLA triblock copolymers were synthesized with different degrees of polymerization ranging from 66 to 333. For the polymer synthesis, the ring-opening polymerization of the hydrophobic monomer l-lactide was used [2]. The polymerization was carried out in the presence of stannous octoate (Sn(Oct)2) as the catalyst. Ring-opening polymerization (ROP) is a type of chain-growth polymerization in which the terminus of the polymer chain attacks the cyclic monomer to form longer polymer chains. The successful synthesis of the polymers was verified by gel permeation chromatography (GPC) whereas their composition was determined by proton nuclear magnetic resonance (^{1}H NMR) spectroscopy.

In the second part of this thesis, the amphiphilic copolymers were self-assembled in water to form either micellar or vesicular structures, able to encapsulate small hydrophobic molecules [3]. Therefore, nanocarriers with two different methods were prepared. The first method includes the dissolution of the polymer in an organic solvent followed by the dropwise addition of the aqueous phase. In the second technique, the thin-film hydration method was used. In this process, the polymer is dissolved in an organic solvent followed by the evaporation of the solvent and the formation of a polymeric film. The film is then hydrated resulting in the self-assembly of the polymeric chains. The size of the nanoparticles was determined by dynamic light scattering (DLS) and their morphology was confirmed by scanning electron microscopy (SEM) and transmission electron microscopy (TEM). Next, the release profile of a model dye, Sudan Red, loaded within the nanoparticles to simulate the hydrophobic drug, was studied. The release kinetics were monitored by UV/Vis spectroscopy. The experimental results showed a slower release of Sudan Red, from mixed diblock and triblock copolymer micelles, reaching a 60% release after 14 days.

Chapter 1: Introduction

1.1. Drug delivery

Drug delivery systems (DDSs) are systems or devices that enable the introduction of a therapeutic substance in the body and improve its efficacy and safety by controlling the rate, time, and place of release of the drug in the body [4]. The administration of these products can be achieved by oral, rectal or transnasal administration. In addition, widely used techniques include intravenous and subcutaneous injections. There is a constant evolution of the delivery methods in order to improve the effectiveness of administrated drugs. One aspect of the topic is related to the release rate of the drug. The sustained release of the pharmaceutical product can prolong its activity in the system and reduce the frequency of dosing [4]. A great deal of research has been also carried out, aiming to control the release of drug molecules by targeting specific organs or cells in the body [5],[6]. Nanocarriers such as liposomes, nanoparticles and micelles have been used for the sustained and targeted drug delivery of therapeutic agents [7], [8].

1.2. Ocular drug delivery

Efficient ocular drug delivery has been a great challenge for scientists due to the existence of unique anatomical and physiological barriers in the eye. These barriers include the tear film, the aqueous humor as well as the sclera, choroid and vitreous body. The barriers lead to fast drug elimination or low absorption from the eye, thus frequent administrations are required. The treatment for ocular diseases includes invasive and non-invasive methods (**Fig. 1.1**). Invasive treatments, like intraocular injections, surgery and laser therapy, are usually accompanied by complications, such as inflammation, high intraocular pressure, retinal hemorrhage and potential visual loss. Non-invasive therapies include oral medications, eye ointments and topical eye drops. Even though these methods have been widely used to treat various diseases, their sort life-time in the eye limit their clinical applications [6]. Recent developments in nanotechnology offer new opportunities to address the limitations of traditional drug delivery systems by developing nanostructures capable of encapsulating and

transporting small molecules. Nanoparticles are defined as structures with sizes in the range of 1–1000 nm. The size of these particles should be less than 10 µm to avoid a foreign body sensation after administration [9]. Potential candidates as drug carriers overcoming the problem of frequent administrations, are nanoparticles (NPs) comprising biodegradable polymers. The NPs can protect the drug from the proteins in the bloodstream, thereby increasing its half-life. They can also slow down the release profile of the drugs and as a result reduce the need for repeated dosing.

.

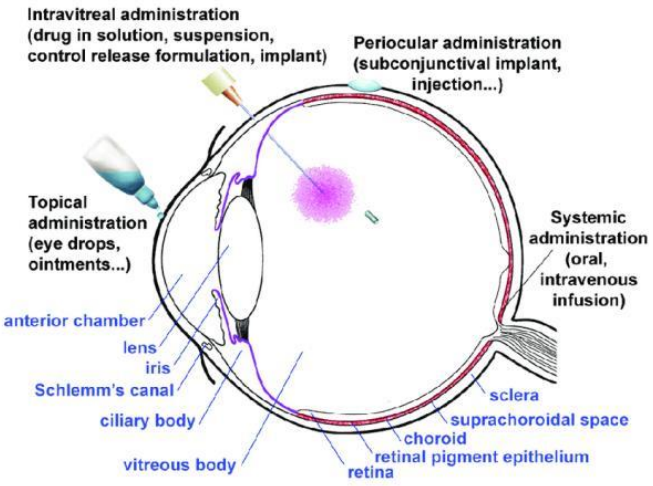

Fig. 1.1. The anatomy of the eye and various routes for drug administration. Adapted from ref. [10].

1.3. Types of nanocarriers

Since 1960, various nanocarriers have been extensively studied for the delivery of drugs. Liposomes, polymeric micelles, vesicles, polymer-drug conjugates are just some of them (**Fig.1.2.**)

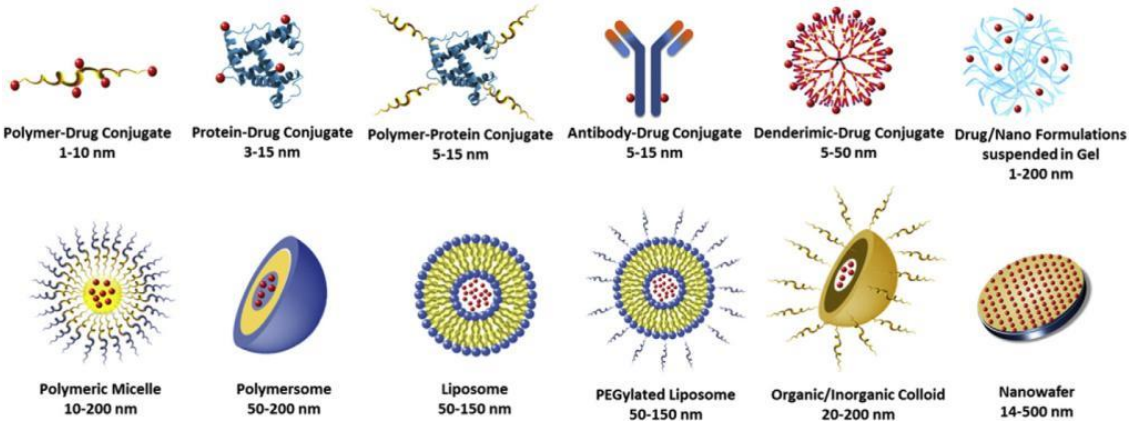

Fig.1.2. Schematic depiction of the most relevant nanomedicine formulations for ocular delivery [1].

1.3.1 Liposomes

Liposomes are tiny "bubble-like" structures with a phospholipid bilayer like a cell membrane, and is capable of caring hydrophilic or lipophilic drugs. Liposome are the most popular and well-studied vehicles for drug delivery. In addition, the liposome surface can be modified by attaching poly(ethylene glycol) chains onto the bilayer to enhance their circulation time in the bloodstream. A study by Karn et al., showed that liposomes loaded with cyclosporine A (CsA), a drug for dry eye syndrome treatment, cause reduced irritation to the eye and are more effective compared to commercial products [11].

1.3.2 Polymeric nanoparticles

Polymeric nanoparticles (NPs) have several advantages over liposomes, including their increased stability and ability of achieved a sustained drug release. Poly(lactic-co-glycolic acid) (PLGA), is a copolymer of poly(lactic acid) (PLA) and poly(glycolic acid) (PGA) which is widely used in the biomedical field in various applications such as surgical sutures, tissue engineering scaffolds and drug delivery systems [12].PLGA is an FDA approved materials, it is biodegradable and its mechanical properties can be adjusted by altering the PLA/PGA ratio and the molecular weight. PLGA NPs have the ability to target specific regions or cells [13] and encapsulate different drugs [14]. *Cañadas et al* explored the effectiveness of

PLGA NPs as a delivery system of pranoprofen within the cornea. Nanoparticles encapsulating pranoprofen exhibited a quick anti- inflammatory action and prolonged retention time on the cornea exterior ,while drastically reducing ocular edema [15]. Another example is chitosan-based nanoparticles. Chitosan is a polysaccharide comprising glucosamine and N-acetylglucosamine units and is obtained by the deacetylation of chitin derived from crustacean shells. In ophthalmic drug delivery, chitosan has great penetration of the corneal surface owing to its mucoadhesive properties [16]. Previous studies have investigated the potential use of chitosan-based NPs for ocular drug delivery [17],[18].

1.3.3 Polymeric micelles

Micelles are spherical structures formed by the self-assembly of amphiphilic molecules in a selective solvent. Above a certain concentration - known as the critical micelle concentration (CMC) - hydrophobic interactions drive the amphiphilic molecules to self-assemble in an aqueous environment (**Fig1.3**). CMC is the minimum concentration of the molecules required for micelles to form. These structures consist of a hydrophobic core and a hydrophilic shell and their typical size is in the range of nanometers [19]. Amphiphilic diblock copolymers are able to self-assemble into polymeric micelles, in which the hydrophobic blocks form the inner core, while the hydrophilic chains expand in the water to form the corona or shell of the micelles [3].

Among the most extensively studied biodegradable block copolymer that can self-assemble into polymer micelles are poly(ethylene glycol)-poly(propylene glycol) (PEG-PPG) [20],[21], poly(ethylene glycol)-poly(ε-caprolactone) (PEG-PCL) [22],[23] and poly(ethylene glycol)-poly(L-lactide) (PEG-PLLA). PLLA is a synthetic hydrophobic polyester with low degradation rate that has been appropriately modified to obtain an amphiphilic polymer [24]. One option is the use of PEG chains which are hydrophilic and biocompatible to form PEG-PLLA and PLLA-PEG-PLLA diblock copolymers [2],[25]. In an aqueous solution, the polymeric chains can self-assemble into micellar nanostructures. These micelles comprise a hydrophobic core consisting of the PLLA blocks and a hydrophilic shell formed by the PEG block. The core can serve as a reservoir for lipophilic drugs, whereas the shell stabilizes the micelles in the

medium [5].PEG-PLLA diblock and triblock copolymers have been investigated for use in drug delivery and tissue engineering [5],[26],[27].

The formation of the polymer micelles can be induced by two main methods. The first is the non-selective-selective solvent method, in which the copolymer is dissolved in a good solvent for both blocks, followed by the addition of water as a selective solvent into the solution. This method leads to the formation of micelles with a uniform size and low polydispersity. The second method involves the dissolution of the polymer in an organic solvent, which is then evaporated to form a polymer film. The film is then hydrated, using an aqueous solvent, resulting in the formation of the polymer nanostructures.

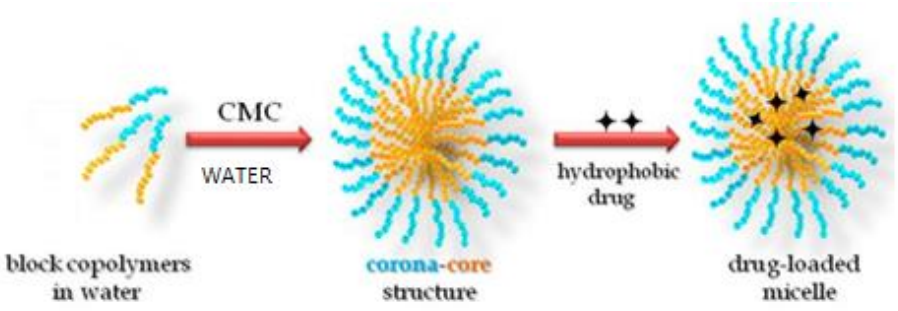

Fig. 1.3. Schematic of the micellization of diblock copolymers and the encapsulation of drug molecules [3].

1.3.3.1 Characteristics of the micelle morphology

The hydrophilic blocks of the amphiphilic copolymers form the shell of the micelles. The shell of the micellar structure determines the charge, lipophilicity, and the size of the micelles. These characteristics play an important role on the biological properties of carriers, such as the biocompatibility, pharmacokinetics and circulation time in the blood. [28]. A variety of parameters affect the micellar morphology. The most important factors are the CMC, the packing parameter and the aggregation number. The process of micelle formation in aqueous solution is driven by hydrophobic interactions between the hydrophobic blocks of the copolymer and the solvent. The balance between the hydrophobic and the hydrophilic parts of the copolymers greatly affects the size of the micelles and the drug loading capacity. Increased hydrophobicity leads to a lower CMC which enhances micelle formation, resulting in

more stable micelles [29]. The value of the CMC mainly depends on the hydrophobic and hydrophilic ratio and is also influenced by the polymer-solvent interactions which can be altered by parameters such as the solution temperature and pH. The primary factor that is responsible for the morphology of micelles is the packing parameter. The packing parameter is defined as

$$p = \frac{v}{a_0 * l_c}$$

where a_0 is the contact area of the hydrophilic group, l_c and v are the length and the volume of the hydrophobic block respectively. For p<1/3, spherical micelles are formed, for 1/3<p>1/2 cylinders are obtained and for 1/2 <p<1 vesicles are formed [30].

The number of polymer chains that assemble to form a micelle is the so-called aggregation number. The aggregation number strongly depends on the chain length and the ratio of hydrophobic and hydrophilic segments of the copolymer [31].

1.4. Mechanisms of drug release from polymeric micelles

Drug release refers to the transportation of a drug molecule from the polymeric micelle to its exterior and into the surrounding environment [32]. In **Fig. 1.4** we can observe the main release mechanisms of drug release: polymer degradation, passive diffusion of the encapsulated molecules and combination of the two [33]. Degradation of the polymeric chains leads to destabilization of the micelles, resulting in the release of the drug (**Fig. 1.4a**). In **Fig. 1.4b**, the drug molecules simply diffuse through the micelle and into the surrounding medium. Finally, in **Fig. 1.4c** we can see the release from a combination of both diffusion and the degradation of the polymer. The release process of the drug can be divided into two phases: in phase 1, the drug molecules quickly diffuse to the medium as a result of the drug absorption onto the surface of the nanocarriers. This phase is known as the burst release phase. In phase 2 (controlled release phase), the mechanism of the release depends on the characteristics of the polymeric system. Diffusion is the main process when the rate of drug diffusion is greater than that of polymer degradation, else polymer degradation is the driving force of drug release [34].

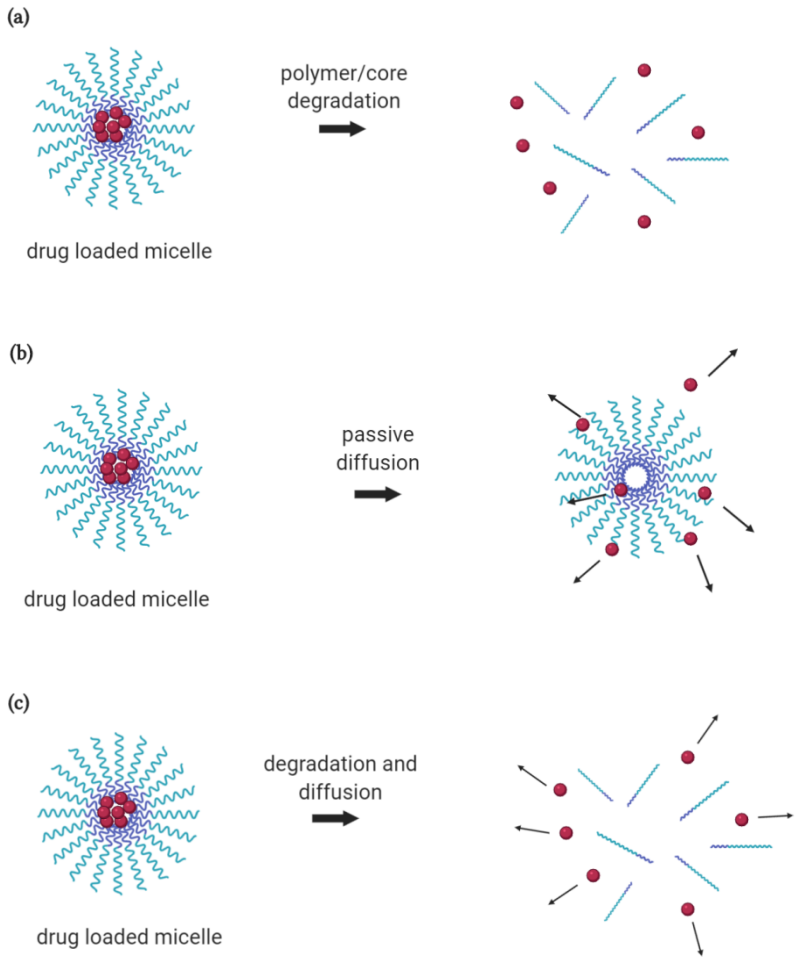

Fig. 1.4. Schematic of release mechanisms from drug loaded micelles by a) degradation of the polymeric chains, b) diffusion of the drug molecules c) a combination of degradation and diffusion. Created with BioRender.com

1.4.1. Factors affecting drug release

Many factors can affect the release behavior of drugs from polymeric micelles. The higher the molecular weight, the larger the size of the micelles which slows down the release rate. The length of the hydrophilic and the hydrophobic blocks of the copolymer also greatly influence the release of the drug molecules. The larger the hydrophobic-to-hydrophilic ratio (the longer the hydrophobic chain), the bigger the micelle core which increases the drug loading capacity [22]. An *in vitro* study by Yang et al. showed that copolymers with longer PLA chain length form tightly packed micelles due to the hydrophobic interactions among the drug molecules and the PLA

chains, thus leading to a slower release rate of the drug from the micelles [35]. Finally, the process of micelle preparation can influence the size, the shape, the drug loading capacity and the stability of the nanocarriers and as a result, the rate and the degree of drug release [36]. Other factors that play an important role in the drug release include the copolymer concentration, the solution pH and the solvent [37].

1.5. Ring Opening Polymerization (ROP)

According to IUPAC, ring opening polymerization is a form of polymerization of cyclic monomers to form acyclic or with fewer cycles polymers [38]. A polymer chain acts as a reactive center and attacks a cyclic monomer, resulting in an acyclic chain and initiating the polymerization of the next monomer. The active polymeric chain can be anionic, cationic or radical. Some of the advantage of this process is its living nature and its capability of producing high molecular weight polymers with controlled polydispersity index (PDI) [39]. ROP requires catalysts in order to proceed. Metal –catalysts, such as lead, aluminum, zinc as well as yttrium and bismuth salts, have been used to produce PLLA industrially. The most widely used metal-complexes are tin(II) 2-ethylhexanoate or stannous octoate ($Sn(Oct)_2$). **Fig. 1.5** illustrates the general scheme of ring-opening polymerization.

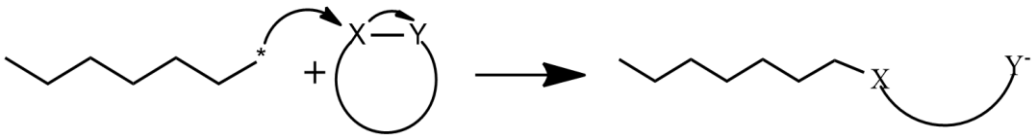

Fig. 1.5. General scheme of ROP. The * refers to anionic, cationic or radical chain.

Chapter 2: Experimental

2.1 Materials

Poly(ethylene glycol) methyl ether (MePEG) with molecular weight of 5000 gr/mol was purchased from Polysciences Inc. MePEG with 2000 gr/mol molecular weight was purchased from Sigma-Aldrich. PEG of 4000 and 1500 gr/mol molecular weight, L-lactide and stannous octoate (95 %) as the catalyst were obtained from Sigma-Aldrich. Sudan Red 7b was used as a model drug and was obtained from Sigma-Aldrich. Tetrahydrofuran (THF) (HPLC grade ≥ 99.9%), methanol and petroleum ether were purchased from Scharlau S. L. THF was purchased from Carlo Erba Reagents and deuterated chloroform (≥ 99.8%) was obtained from Deutero GmbH. Finally, dichloromethane (≥ 99.9%) and toluene (≥ 99.9%) were purchased from Sigma-Aldrich. Milli-Q water with a resistivity of 18.2 MΩ.cm at 298 K was obtained from a Millipore apparatus and was used for all experiments

2.2 Synthesis of poly(ethylene-glycol) methyl ether-*b*-poly(L-lactide) (MePEG-*b*-PLLA) diblock copolymers and PLLA-*b*-PEG-*b*-PLLA triblock copolymers

The synthesis of MePEG-*b*-PLLA copolymers was achieved through a ring-opening polymerization of L-lactide using MePEG as the initiator and $Sn(Oct)_2$ as the catalyst. Briefly, a pre-determined amount of freeze-dried MePEG, recrystallized L-lactide and the catalyst were added into the reaction vessel. Then, the vessel was placed inside an oil bath at 130 °C for 24 hours under stirring. The reaction was carried out under a nitrogen atmosphere. Afterwards, the final product was dissolved in dichloromethane and was precipitated in petroleum ether. The supernatant was disposed and the product was left under vacuum to dry. The same procedure was followed for the synthesis of the PLLA-*b*-PEG-*b*-PLLA triblock copolymers. The experiment was repeated using different molecular weights of PEG and different targeted molecular weights of PLLA. The products were characterized by GPC and ^{1}H NMR spectroscopy.

2.3. Preparation of the PEG-*b*-PLLA and PLLA-*b*-PEG-*b*-PLLA nanocarriers

The nanocarriers where prepared by two different methods, the non-selective-selective solvent dissolution method and the thin film hydration. In the first method, 20 mg of the polymer were dissolved in 2 ml of THF. Then 10 ml of milli-Q water (pH 7.4) were added using a syringe pump at a rate of 0.1 ml/min. Next, the organic solvent was evaporated under vacuum using a rotary evaporator. Finally, the solution was filtered through a hydrophilic Chrompure PVDF/L filter with 0.45 μm pore size and was stored in the fridge until use. For the thin film hydration method, 20 mg of the polymer were dissolved in 2 ml of methanol and the solvent evaporated under vacuum, creating a thin polymeric film on the walls of the round bottom flask. Finally, water was added into the flask and the film was slowly hydrated, leading to the micellization of the polymer. The size of the nanocarriers was determined by dynamic light scattering (DLS) and their morphology was confirmed by field emission scanning electron microscopy (FESEM) and transmittance electron microscopy (TEM).

2.4. Release studies

The release behavior of the polymeric micelles, loaded with a hydrophobic dye, Sudan Red 7b, was studied. A stock solution of Sudan Red 7b with concentration 2 mg/ml was prepared in THF. The encapsulation of the dye was achieved using the non-selective-selective solvent dissolution technique. Briefly, 200 μl of stock solution were added in the polymer solution and the same procedure as that described above for the polymeric micelles was followed. To study the release profile, 5 ml of the above sample were added in a vial and were placed inside a water bath at a constant temperature of 37 °C, to simulate the body temperature. At predetermined time intervals, 3 ml of the sample were measured using UV/vis spectroscopy and the absorption of the dye inside the micelles was recorded at 535 nm. The % release of the dye was calculated using the follow equation:

$$\%\text{Release} = \frac{A_0 - A_t}{A_0} * 100\%,$$

Where, A_o and A_t is the absorbance of the sample at time zero and t (each time interval), respectively

2.5 Characterization methods

2.5.1 Gel Permeation Chromatography (GPC)

In order to determine the molecular weights and the PDIs of the polymers, GPC was used, equipped with a Waters-515 isocratic pump, two columns, Mixed-D and Mixed-E (Polymer Labs), a Waters 2745 Dual Absorbance detector and a Waters 410 refractive index (RI) detector. THF (HPLC grade) with 2 v/v% TEA was used as the eluent at a flow of 1 mn/min and the column temperature was set at 25 C. Usually 20-30 mg of the polymer were dissolved in 1ml THF (HPLC). Next, the solution was filtered using a PTFE filter with 0.45 μm pore size and was consequently injected into the system. The molecular weight of the polymer was calculated using a calibration curve based on PMMA standards with molecular weights ranging from 625-138600 gr/mol.

2.5.2 Proton Nuclear Magnetic Resonance (^{1}H NMR) spectroscopy

The polymers where characterized by ^{1}H-NMR spectroscopy on an Avance Bruker 300 MHz spectrometer with tetramethylsilane (TMS) as an internal standard and $CDCl_3$ as the solvent.

2.5.3 Field emission scanning electron microscopy (FE-SEM)

FESEM images were obtained using a JEOLJSM-7000F microscope. A drop of the sample was deposited on a glass panel and was left to dry overnight at room temperature. Then the sample was sputter-coated with Au (10mm thick) before imaging.

2.5.4 Dynamic Light Scattering (DLS)

The size of the micelles was measured using a Malvern Zetasizer Nano ZS instrument equipped with a 4 MW He-Ne laser operating at λ = 632.8 nm. The scattering angle was 90° and three scans were collected for each measurement. The sample concentration was 1 mg/ml.

2.5.5 Transmission Electron Microscopy (TEM)

TEM images were captured with a JEOL JEM-2100 instrument at 80 KV. A drop of the sample was deposited on a carbon-coated cooper grid and was left to dry overnight.

2.5.6 Ultraviolet/Visible spectroscopy

The UV/Vis absorption spectra were recorded using a Lambda 25 spectrophotometer (Perkin Elmer) in the wavelength range of 200-700 nm. The samples were measured in quartz cuvettes

2.6 Characterization techniques

2.6.1. Gel Permeation Chromatography (GPC)

Gel permeation chromatography (GPC), or size exclusion chromatography (SEC), is a well-known polymer separation method that allows determination of the polymer molecular characteristics, such as the average molecular weight and molecular weight distribution. In general, GPC is an important analytical tool used to evaluate the molecular characteristics of natural or synthetic polymers and proteins. A GPC instrument comprises a pump, a detector (e.g. UV or RI or both) and one, two or more separating columns. The columns or the stationary phase are filled with porous beads such as polystryrene gels. The beads are made with a variety of pore sizes that span the range of the sizes of the macromolecules to be separated. The pump circulates solvent (mobile phase) through the gel columns and swells the gel material in the

column. A small amount of diluted polymer solution in the same solvent as the mobile phase is injected in the flowing solvent entering the columns. As the polymer solution passes through the columns, the largest polymer particles are excluded from all, but the largest pores and elute from the column first. Right after, smaller polymer coils can pass through smaller pores and are excluded later from the columns. In this way, GPC separates the molecules by their size in solution, which is their hydrodynamic volume (V_h). After separation, the solution passes through the detectors used in the system and are analyzed, upon proper calibration with narrow molar mass distribution standards.

2.6.2 ^{1}H NMR spectroscopy

NMR spectroscopy is a very useful technique commonly employed for the determination of the chemical structure of chemical compounds. ^{1}H NMR and ^{13}C NMR are most commonly used for the characterization of materials. NMR is a spectroscopic technique allowing to observe local magnetic fields around atomic nuclei. The sample with the material is placed in a magnetic field and the NMR signal is produced by excitation of the nuclei of the sample with radiowaves into nuclear magnetic resonance, which is detected with sensitive radio receivers. The signal provides the required information regarding the environment of the nuclei. The exact field strength (in ppm) of a nucleus comes into resonance relative to a reference standard, usually the signal of the deuterated solvent used. Electron clouds shield the nuclei from the external magnetic field causing them to absorb at higher energy (lower ppm), while the neighboring functional groups “deshield” the nuclei causing them to absorb at lower energy (higher ppm). Chemically and magnetically equivalent nuclei resonate at the same energy and give a single signal or pattern. Protons on adjacent carbons interact and split each other’s resonances into multiple peaks following the n+1 rule with coupling constant J. Spin-spin coupling is commonly observed between nuclei that are one, two and three bonds apart. The area under an NMR peak is proportional to the number of nuclei that give rise to that resonance, thus by integration, the protons of that resonance can be calculated.

2.6.3. UV/Vis spectroscopy

UV/Vis spectroscopy is a commonly used technique for the characterization and analysis of both organic and inorganic materials. It is also used for the quantitative determination of loaded molecules within nanoparticles. The range of wavelengths that correspond to the UV/Vis spectrum is from 200 to 800 nm, from which 200-400 nm is the ultraviolet region and 400-800 nm is the visible region. When organic molecules that contain π-electrons are strike by UV/Vis light, then the molecules absorb this energy and electronical transitions occur. The absorbance A can be defined by the Beer-Lambert law that correlates the absorption with the concentration of the absorbing species as shown in the equation below:

$$A = \log10 (I_0/I) = \varepsilon * L * c$$

Where, (I_0) is the intensity of the incident light, (I) is the intensity of the transmitted light, (ε) is the absorption coefficient, which is constant for a specific substance and depends on the wavelength, the solvent and the temperature, (L) is the path length through the sample and (c) is the concentration of the sample

2.6.4 Dynamic Light Scattering (DLS)

Light scattering is a powerful tool for the characterization of the size of polymer nanoparticles in solution. The monochromatic, coherent laser beam hits the particles, and is scattered, due to the Brownian motion of the particles that changes their distance in the solution, and a time-dependent fluctuation of the scattering intensity is observed. By changing the observation angle (θ) and thus the scattering vector (q) a measure of the particle size is provided. The form factor, that is the interference pattern of the scattered light, is characteristic of the size and shape of the scatterers. The larger the particles are the slower their Brownian motion. Accuracy and stability of the temperature during the entire measurement is essential since the viscosity of the liquid is related to the temperature.

The velocity of the Brownian motion is defined by the translational diffusion coefficient (D). The Stocks-Einstein equation is used to calculate the particles' size based on the translational diffusion coefficient:

$$R_h = \frac{K_B T}{6\eta\pi D}$$

Where, (R_h) is the hydrodynamic radius, (η) is the viscosity of the solvent, (K_B) is the Boltzmann constant and (T) is the temperature.

2.6.5 Field Emission Scanning Electron Microscopy (FESEM)

Scanning electron microscopy is designed to provide high-resolution images of a sample placed on a surface. A tungsten filament emits electrons, which are focused by an electron optical system. The electron beam can scan the sample surface and can provide its composition at a point, along a line or over a rectangular area, by scanning the beam across the surface in a series of parallel lines. The sample is mounted on a stage that can be accurately moved in all three directions (x, y and z), normal to the plane of the sample. The instrument generally operates under high vacuum in a very dry environment in order to produce the high energy beam of electrons needed for imaging. However, most specimens destined for study in the SEM are poor conductors. In SEM, the imaging system depends on the specimen being sufficiently electrically conductive to ensure that the bulk of the incoming electrons go to ground. The formation of the image depends on the collection of the different signals that are scattered as a consequence of the high electron beam interacting with the sample. The two principal signals used to form images are backscattered and secondary electrons generated within the primary beam-sample interactive volume. The backscattered electron coefficient increases with increasing the atomic number of the specimen, whereas the secondary electron coefficient is relatively insensitive to the atomic number. This fundamental difference in the two signals has an important effect on the way samples may need to be prepared. The use of scanning electron microscopy may be considered when being able to interpret the information obtained from the SEM, and attempt to relate the form and structure of the two-dimensional images and the

identity, validity and location of the chemical data, back to the three-dimensional sample from which the information was derived. The biggest difference between a FESEM and a SEM lies in the electron generation system. As the source of electrons, FESEM uses a field emission gun that provides extremely focused, high- and low-energy electron beams, which greatly improves spatial resolution and enables work to be carried out at very low potentials (0.02–5 KV). This helps to minimize the charging effect on non-conductive specimens and to avoid damage from the electron beam on sensitive samples.

2.6.6. Transmission Electron Microscopy (TEM)

In TEM, the beam of electrons from the electron gun is focused into a small, thin, coherent beam by the use of the condenser lens. This beam is restricted by the condenser aperture, which excludes high angle electrons. The beam then strikes the specimen, and electrons are transmitted depending upon the thickness and electron transparency of the specimen. The transmitted portion is focused by the objective lens forming an image on a phosphor screen or a charge coupled device (CCD) camera. Optional objective apertures can be used to enhance the contrast by blocking out high-angle diffracted electrons. The darker areas of the image represent the areas of the sample where fewer electrons are transmitted, while the lighter areas of the image represent the areas of the sample where electrons were transmitted through.

Chapter 3: Results and Discussion

3.1 Synthesis and characterization of PEG-*b*-PLLA diblock and PLLA-*b*-PEG-*b*-PLLA triblock copolymers

PEG-*b*-PLLA diblock and PLLA-*b*-PEG-*b*-PLLA triblock copolymers were successfully synthesized by ring-opening polymerization. **Fig. 3.1a** shows the schematic representation of a polymerization for the synthesis of the PEG-*b*-PLLA deblock copolymer, whereas **Fig. 3.1b** shows the synthesis of the triblock copolymers. Briefly, the polymerization of the monomer, L-lactide, started with PEG as the initiator. In the case of the diblock copolymer, the polymerization starts from the hydroxyl group of MePEG. In the case of the triblock, a bifunctional PEG was used. The hydroxyl groups from both ends of PEG acted as initiators and the polymerization of L-lactide started from both sides.

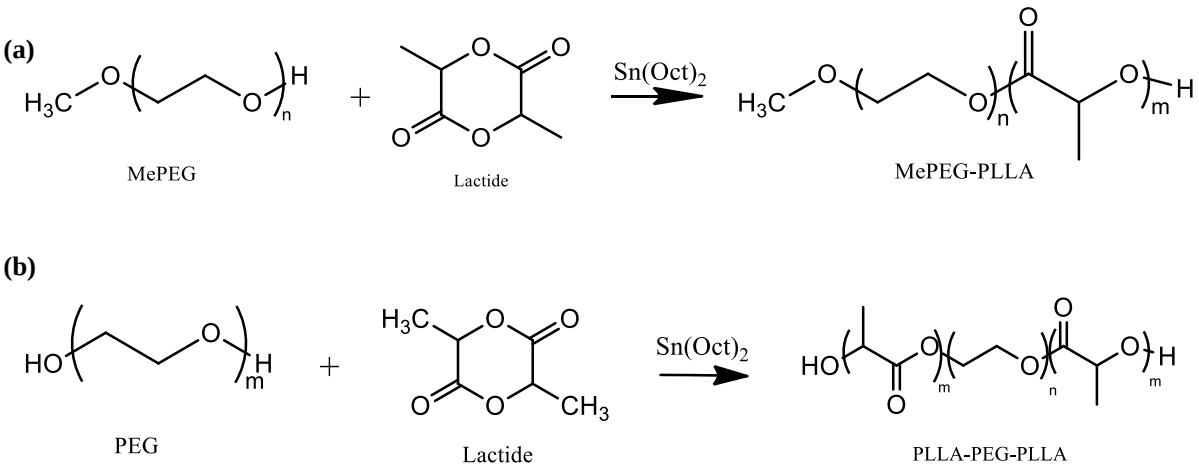

Fig. 3.1. Synthesis of (a) PEG-*b*-PLLA diblock copolymer and (b) PLLA-*b*-PEG-*b*-PLLA copolymer.

The successful synthesis of the copolymers was verified by GPC. **Figure 3.2** shows typical chromatograms of the PEG-*b*-PLLA diblock copolymers. More specifically, **Figs. 3.2a and b** show the copolymers using PEG with a molecular weight of 5000 gr/mol as the macroinitiator. As the molecular weight of the polymer increases, the GPC curve is shifted to lower elution times. The GPC curves of the copolymers and

PEG slightly overlap, which indicates the successful block copolymer synthesis and, in most cases, the absence of PLLA homopolymer peaks is observed. In the case of D5-15 (**Fig. 3.2b**), a small peak can be observed at higher elution times. This indicated the formation of PLLA homopolymer which could be attributed to the presence of traces of humidity in the reaction that can initiate the ROP of L-lactide. In addition, the higher PDI of the polymer is also a result of the homopolymerization of the monomer.

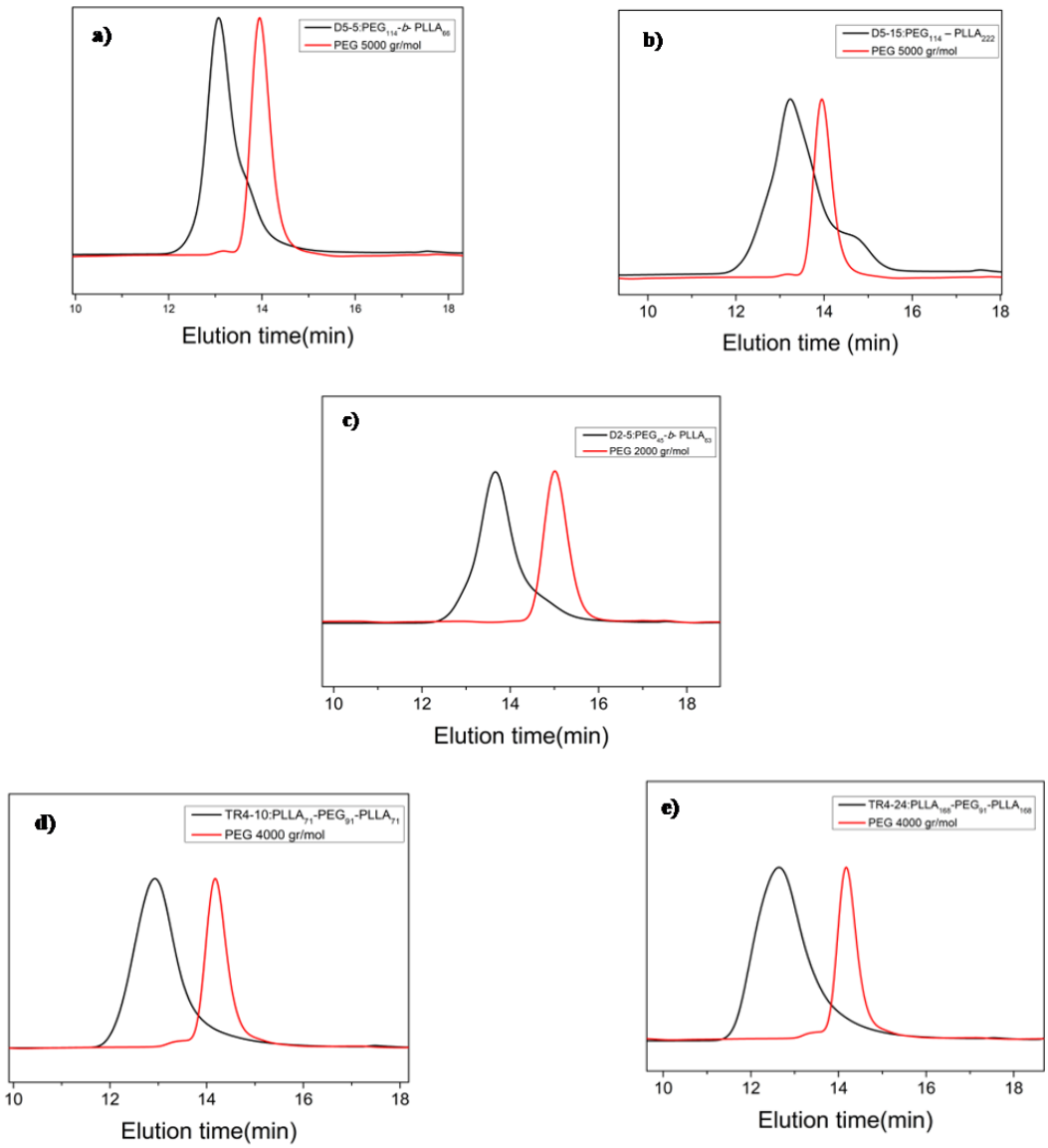

Fig. 3.2. GPC traces of (a) D5-5 (b) D5-15 and (c) D2-5 diblock copolymers and the (d) TR4-10 and (e) TR4-24 triblock copolymers.

The chemical structure and the composition of the diblock and triblock copolymers were determined by ^{1}H NMR spectroscopy. **Figure 3.3a** shows the NMR spectrum of a diblock copolymer. The peak at 1.6 ppm (a) is assigned to the 3 protons of the methyl group of the L-lactide monomer repeat unit, the peak at 5.18 ppm (b) refers to the proton of the –CH group of the lactide units, while the peak at 3.67 ppm (c) is assigned to the 4 protons of the PEG block. Similar, for the triblock copolymer, the peak of the methyl group of the L-lactide monomer repeat units at 1.58 ppm (a), the peak of the proton of the –CH group of the lactide units at 5.19 ppm (b), and the 4 protons of PEG at 3.67 ppm (c), are observed (**Fig. 3.3b**). By defining the number of hydrogen atoms in the product which are assigned to PEG, and integrating the relevant peaks, we can calculate the number of protons assigned to PLLA, and thus determine the molecular weight of the diblock and triblock copolymers.

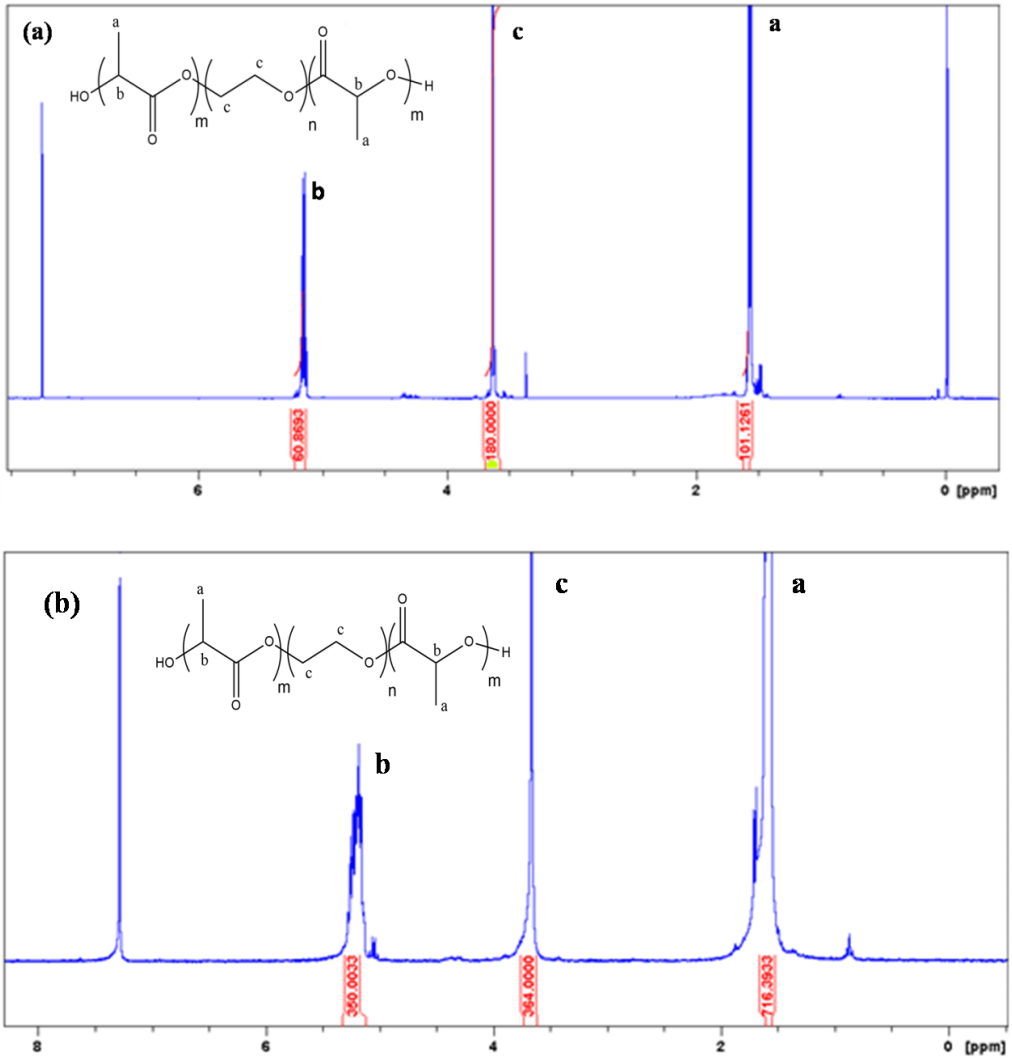

Fig. 3.3. ^{1}H NMR spectrum of (a) a diblock copolymer and (b) a triblock copolymer in $CDCl_3$

Table 3.1 shows the molecular weights of the polymers calculated by GPC and ^{1}H NMR spectroscopy, the polydispersity index by GPC, the degrees of polymerization of PEG and PLLA and the conversion of the L-lactide monomer. The conversion was determined by the ^{1}H NMR spectrum of the reaction mixture (data not shown) before the precipitation of the polymer in petroleum ether. The difference in the molecular weight determined by GPC and ^{1}H NMR is attributed to the relative nature of the GPC method, which determines the apparent molecular weight of a polymer based on its hydrodynamic volume and using a calibration curve, whereas ^{1}H NMR spectroscopy gives the absolute value of the polymer molecular weight.

As seen in **Table 3.1**, for low molecular weight polymers, the PDI is relatively low (M_w/M_n = 1.10-1.19), while, as the molecular weight of the copolymer increases, so does the PDI. This is attributed to the non-living nature of the polymerization, which however, allow the synthesis of block copolymers.

Table 3.1. Characterization of diblock and triblock copolymer by GPC and ^{1}H NMR

Polymer D, TR x,y[a]	M_n[b] (gr/mol)	M_w[b] (gr/mol)	$M_{n\ NMR}$ (gr/mol)	PDI	DP PEG	DP PLLA	Conv. (%)
D2-5	6903	8202	7184	1.19	45	69	93.7
D5-5	9695	10667	9824	1.10	114	66	90
D5-15	14336	19464	21056	1.35	114	223	
TR4-24	28500	41604	30496	1.46	91	333	93.5
TR4-10	17140	21972	14224	1.28	91	183	84

[a] D, TR are the abbreviations for diblock and triblock, respectively and x, y denote the molecular weights of PEG and PLLA (in Kg/mol), respectively

[b]Determined by GPC analysis with PMMA standards

3.2. Self-assembly of the PEG-*b*-PLLA diblock copolymers

The self-assembly properties of the synthesized diblock copolymers and their ability to self-organize into nanosized carriers were investigated. A lot of research has focused on the study of different micellization methods and how the process affects the size and shape of the micelles [41]. To evaluate this, we prepared nanocarriers with the non-selective-selective solvent dissolute method as well as the thin film hydration (TFH) method and compared the results. With the first method one can prepare micelles of uniform size and low polydispersity [42]. The second method has

been widely used for the preparation of liposomes and polymeric vesicles. Our aim was to prepare polymeric micelles with the first method and polymeric vesicles with the second. **Table 3.2** summarizes the measured sizes of the nanocarriers obtained by the DLS measurements **(Figs. 3.5-3.7)**.

The thin film hydration method produced micelles of smaller size for D5-5 and D2-5 compared to the first method. According to the literature, a longer PLLA block leads to the formation of micelles with a larger hydrophobic core and therefore, micelles of larger size [43]. As seen in **Figs. 3.4a and 3.6** the micelles obtained with D5-5 (28nm) were much smaller in size than those for D5-15 (172nm), since the PLLA block was much longer for the latter copolymer. On the contrary, the micelles obtained for D2-5 were larger than those prepared with D5-5. According to *Gill et al*, higher molecular weight PEG chains tend to form larger in size micelles [44]. This was not the case in this work, since the hydrodynamic diameter of the D2-5 polymeric micelles was 164 nm while, D5-5 formed micelles with a size of 28 nm. This is attributed to the low molecular weight of PEG 2000 g/mol which is not sufficient to confer stability to the micellar structures, and led to the formation of micellar aggregates as seen below in **Figure 3.4a**. Such aggregates were also observed for the D5-5 copolymer micelles, besides the individual micelles (**Figure 3.5a**). The micelles formed and their morphology and sizes were also confirmed by FESEM and TEM (**Figs. 3.4-3.6**). **Figs. 3.4c and Fig. 3.5 c** show TEM images of micellar aggregates from the D2-5 and D5-5 copolymers respectively. These images confirm the spherical structure of the nanosized carriers and the aggregates are in agreement with the second peak in the DLS measurements**. Fig. 3.4b** shows SEM image of D2-5 micelles. The size from the SEM imaging (146 nm) matching the size from DLS (164 nm) and the smaller size is due to the dry nature of the technique and the collapse of the micellar corona.

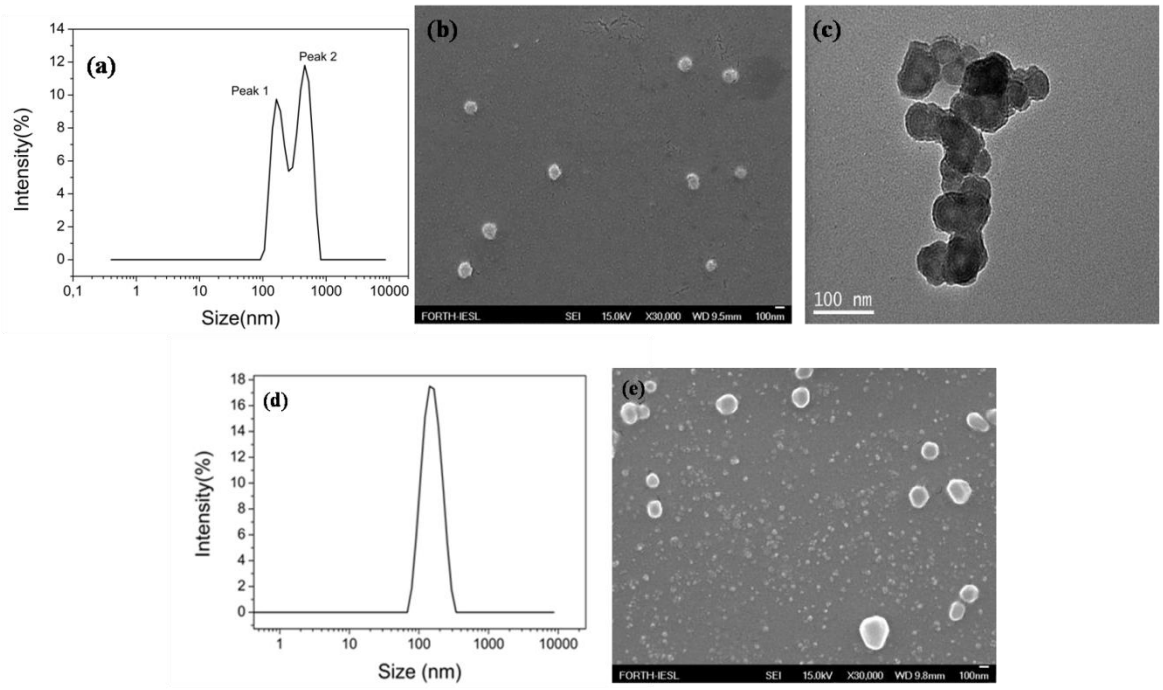

Fig. 3.4. a) DLS measurment of D2-5 micelles b) FE-SEM image of D2-5 micelles c) TEM image of D2-5 micelles d) DLS measurment of D2-5 micelles with TFH e) FE-SEM image of D2-5 micelles with TFH.

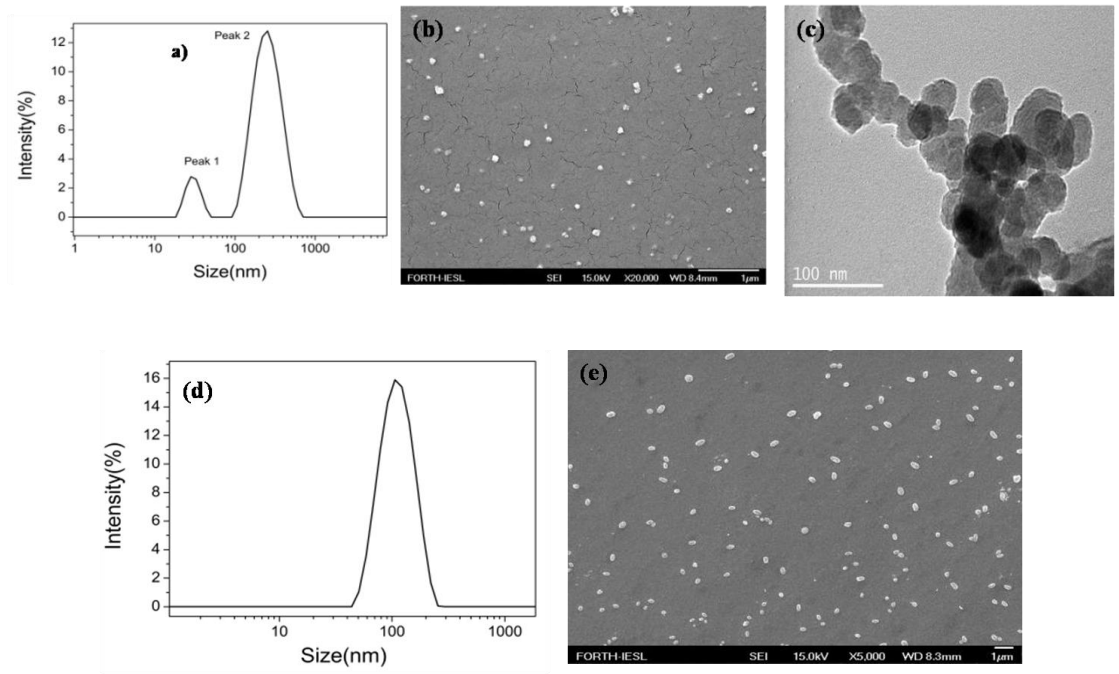

Fig. 3.5. a) DLS measurment of D5-5 micelles b) FE-SEM image of D5-5 micelles c)TEM image of D5-5 micelles d) DLS measurment of D5-5 TFH micelles e) FE-SEM image of D5-5 TFH micelles.

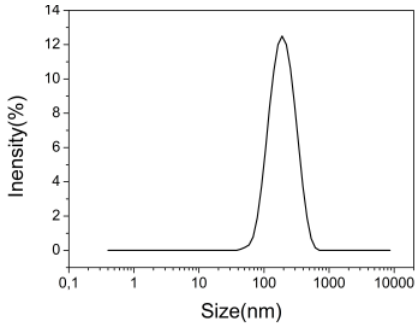

Fig. 3.6. DLS measurment of D5-15 micelles

3.3. Self-assembly of the PLLA-*b*- PEG -*b*-PLLA triblock copolymers

The self-assembly properties of the synthesized triblock copolymers were also studied. Polymers TR4-24 and TR4-10 comprise a PEG mid-block of 4000 gr/mol molecular weight and two PLLA blocks of 24000 gr/mol and 10000 gr/mol molecular weights, respectively. Micelle formation was induced using the non-selective-selective solvent dissolution method to produce micelles of low polydispersity. **Figures 3.7 and 3.8** show the DLS measurments and the FESEM and TEM images of the polymeric micelles. Micelles with an average diameter of 33 nm were formed for TR4-10 and 44 nm for TR4-24. The length of the hydrophobic block plays a crucial role in the micellization process, with the longer PLLA chains forming larger hydrophobic cores and resulting in bigger micelles. However, in the case of the triblock copolymers the micellar sizes are in good agreement with the block lengths possibly due to the block copolymer arhitecture which results in the formation of stable “flower-like” micelles. As previously,FESEM and TEM images confirm the existence of micellar aggregates and the sphere-like shape of the nanocarriers (**Fig. 3.7 c and Fig. 3.8. b**).

Table 3.2. Micellar size of diblock and triblock copolymers from DLS

Polymeric micelles	Size (nm)
D2-5	Peak 1:164 Peak 2: 458
D2-5 TFH	157
D5-5	Peak 1:28 Peak 2:255
D5-5 TFH	111
D5-15	172
TR4-24	Peak 1: 44 Peak2: 220
TR4-10	Peak 1:33 Peak2:220

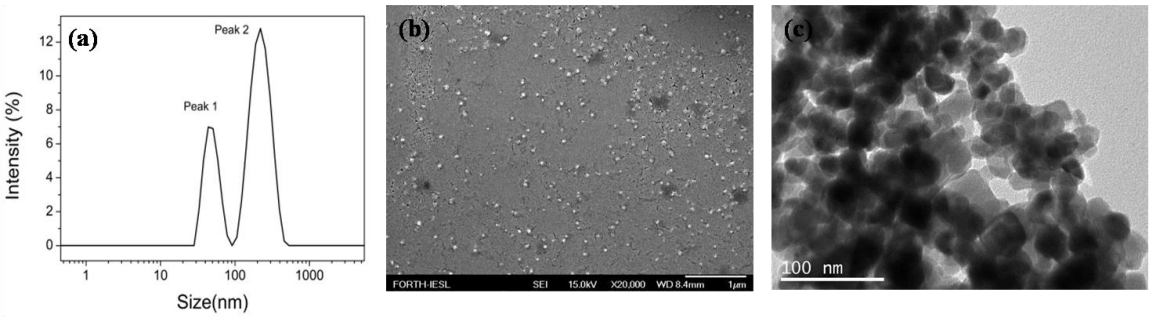

Fig. 3.7. a) DLS measurment of TR4-24 copolymer micelles b) FE-SEM image of TR4-24 copolymer micelles c) TEM image of TR4-24 copolymer micelles.

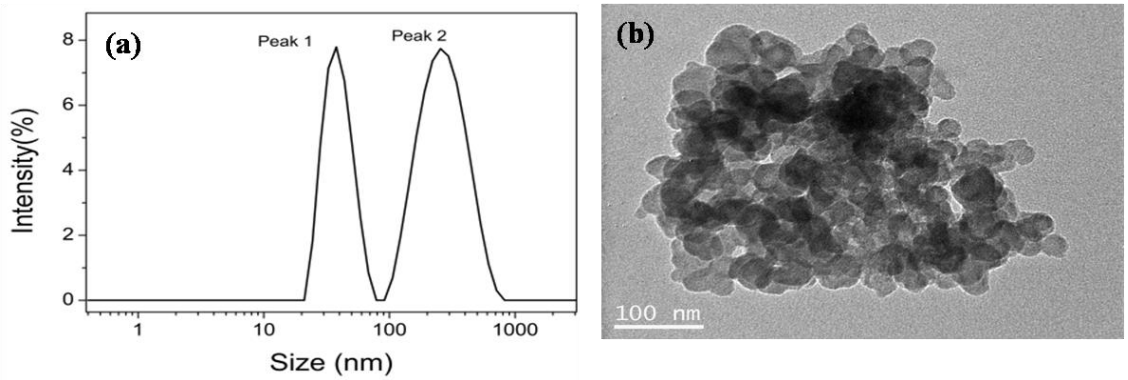

Fig. 3.8. a) DLS measurment of TR4-10 copolymer micelles b) TEM image of TR4-10 copolmer micelles.

3.4. Release studies

The main objective of this study was the development of biodegradable nanocarriers capable to encapsulate hydrophobic drugs and slowly release them over time. In order to study the drug loading ability of the polymeric nanocarriers and their release profiles, the block copolymers D5-5, D5-15, TR4-24, TR4-10 and a mixture of TR4-10 and D5-15 were used. The encapsulation of Sudan Red 7b was achieved using the dissolution method described in the Experimental section.

3.4.1. Release studies of Sudan Red loaded within the PEG-*b*-PLLA diblock copolymer micelles.

Fig. 3.9. shows the UV/Vis spectra of the D5-5 (**Fig. 3.9a**) and D5-15 (**Fig. 3.9b**) micelles loaded with Sudan Red as a function of time. The drug loading of the D5-5 micelles was 0.14%, while the D5-15 micelles had a loading of 0.11%. The absorbance maximum at 535nm of the encapsulated dye within the micelles was measured and was found to decrease over time, indicating the release of the dye from the micelles and the precipitation of the released dye. The process was also verified visually as a change in the color for the solutions from pink to almost colorless. **Fig. 3.9c** shows the % release of the dye as a function of time. As observed, the release of the dye consists of two stages, the first is the burst release during the first few hours of the experiments followed by a second sustained release. The burst release is associated with the amount of dye absorbed onto the surface of the micellar core, whereas, the slow drug release is associated with the dye which is encapsulated within the hydrophobic core of the micelles.

Comparison of the release profiles of the two diblock copolymers showed that the D5-15 micelles, which are bigger in size exhibit a smaller burst release and a slower rate of release rate of the dye compared to the D5-5 micelles with the smaller hydrophobic core. In particular, after 48 h D5-5 exhibited 80% release of the dye, whereas D5-15 a 53% release. It is however, interesting that both micellar samples exhibited a similar release (90%) after 120 h.In addition both of the micellar systems had similar drug loading ability. This indicates that the PEG/PLLA composition plays a vital role in slowing down the release rate from the polymeric micelles in the second stage.

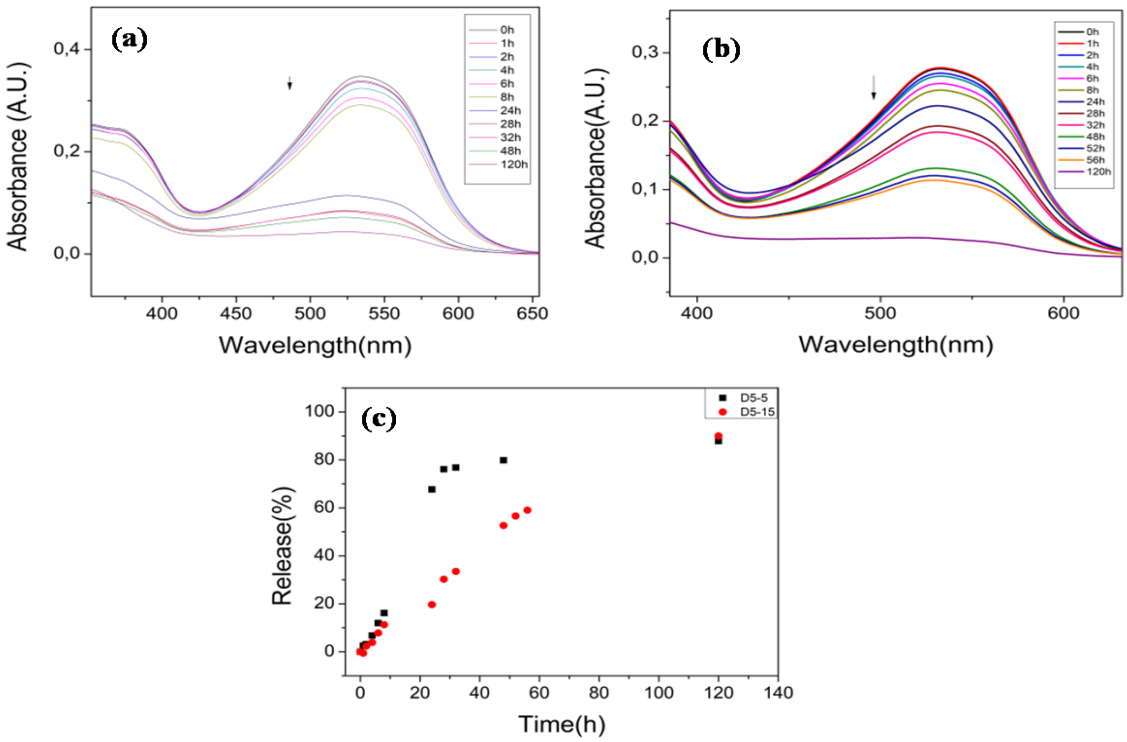

Fig. 3.9. a) UV/Vis spectra of D5-5 loaded copolymer micelles b) UV/Vis spectra of D5-15 loaded copolymer micelles c) comparison of the release percentage of Sudan Red from D5-5 and D5-15 copolymer micelles.

3.4.2. Release study of the Sudan Red loaded within the PLLA-*b*-PEG-*b*-PLLA triblock copolymer micelles.

The triblock copolymers, TR4-24 and TR4-10, were studied in order to investigate the influence of the copolymer architecture on the release rate from the micellar core. The drug loading of TR4-24 micelles was 0.17% whereas the drug loading of TR4-10 was 0.28%. As seen in **Fig 3.10**, the two triblock copolymer micelles exhibited a similar burst release but differed slightly in the second sustained release phase. More specifically, the TR4-24 nanocarriers showed a 95% release in only 2 days, while the TR4-10 copolymer micelles released ~73% of the load for the same time, reaching a plateau in the release profile at this value., This result does not agree with the larger size of the TR4-24 copolymer micelles for which a more sustained release would be expected. This result can be explained from the drug loading of the nanocarriers.TR-4-10 had larger drug loading compared to TR4-24 and as a result it would take longer to release the drug.

When compared to the results from the diblock copolymers, triblock copolymers seem to release their cargo much faster. One reason why this happened is that the nanocarriers from the triblock copolymers had absorbed a large amount of drug onto their surface, thus leading to faster release of the drug molecules.

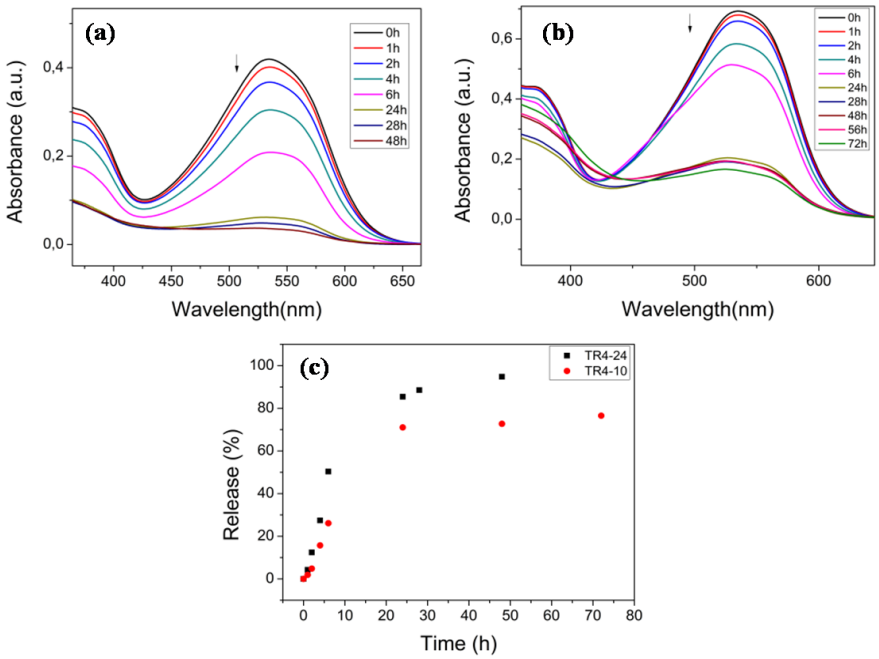

Fig. 3.10. a) UV/Vis spectra of TR4-24 loaded copolymer micelles b) UV/Vis spectra of TR4-10 loaded copolymer micelles c) comparison of the release percentage of Sudan Red from TR4-24 and TR4-10 copolymer micelles.

3.4.3. Release study of Sudan red encapsulated in the TR4-10 and D5-15 mixed micelles

From the above results for the diblock and triblock copolymer micelles, the release kinetics were not sufficiently low. The D5-15 micelles exhibited the slowest release of the dye which lasted for ~5 days. In order to slow down further the release of the dye molecules from the micelles, we prepared mixed micelles comprising the TR4-10 and D5-15 copolymers. We envisage that these copolymers would form a more complex micellar structure with the PEG chains of the diblock copolymers extending in the solution and the hydrophilic mid-blocks of the triblock copolymers forming "loops", in a flower-like structure (**Fig. 3.11**). We also assumed that these micelles

could be more stable, due to their complex structure, and capable of further slowing down the release profile of the dye.

.

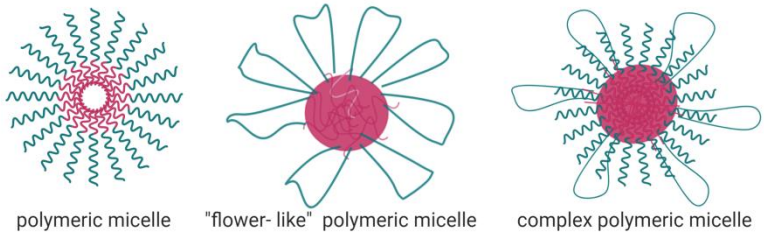

Fig. 3.11. Schematic illustration of the self –assembly of diblock and triblock copolymer nanocarrier

Indeed, the obtained results showed a slower release of the dye, which reached 50% after 6 days (144h) (**Figure 3.12**). Again, a burst release was found for the first few hours of the experiment however the second phase exhibited a more effective sustained release. Due to the complexity of the structure of the nanocarrier and the strong hydrophobic interactions between the micellar core and the dye molecules, the micelles released 58% of their load after 14 days. Therefore, the mixed nanocarriers seem to significantly delay the release of the dye, and, the cumulative release is much lower than the amount released from the diblock or triblock copolymer micelles. These results are very promising and suggest that further work is required to study in detail the potential of the mixed polymeric nanocarriers in drug delivery applications.

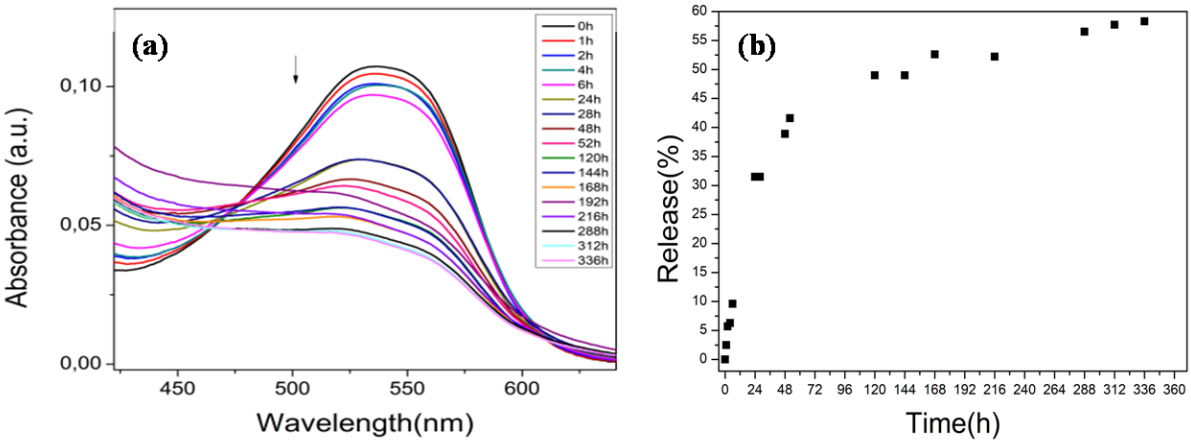

Fig. 3.12. a) UV/Vis spectra of mixture of TR4-10 and D5-15 loaded micelles b) Release profile of the mixture

3.5. Study of the release mechanism from the PEG-*b*-PLLA and PLLA-*b*-PEG-*b*-PLLA copolymer micelles

As mentioned above, the possible release mechanisms of active compounds from diblock copolymer micelles include the diffusion of the dye molecule from the micelles into the surroundings, the degradation of the polymeric nanocarriers and a combination of those.

The release mechanism that operates for the micellar systems used in this study, was studied by ^{1}H NMR spectroscopy. The degradation products expected for the PEG-*b*-PLLA copolymers are LA oligomers, PEG and the monomer lactic acid.

Fig. 3.13 shows the ^{1}H NMR spectra of the D5-5 copolymer micelles before **(a)** and after **(b)** the dye release. The peak at 1.26 ppm **(d)** is assigned to the methyl group of lactic acid[45]. The existence of lactic acid peaks confirms the degradation of the polymeric nanocarriers. From the integrals of the peaks we calculated the degradation percentage, which in the case of D5-5 was 12.5%. As a result, the degradation of the micellar core leads to the release of the drug molecules from the nanocarriers.

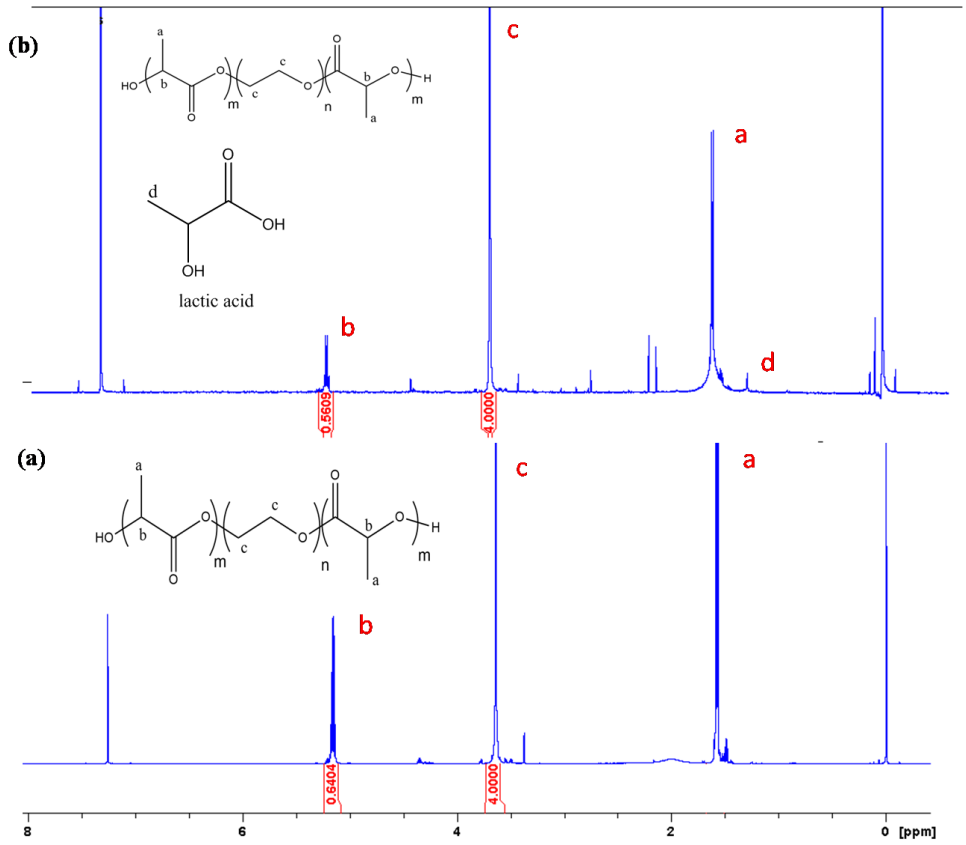

Fig. 3.13. ^{1}H NMR spectra of the D5-5 micelles (a) before and (b) after the dye release study.

Chapter 4: Conclusions and future perspectives

Ocular drug delivery has been a challenge for scientists due the complex structure of the eye. A variety of different nanocarriers, including liposomes, polymeric nanoparticles and polymeric micelles and vesicles, have been used in the past to efficiently deliver pharmaceutical substances. Polymeric micelles comprising biodegradable, amphiphilic block copolymers have been widely used as drug carriers. The main objective of this thesis was the synthesis of biodegradable diblock and triblock copolymers capable to self-assemble into micellar structures for use in ocular drug delivery.

PEG-*b*-PLLA and PLLA-*b*-PEG-*b*-PLLA copolymers were synthesized and were characterized by GPC and ^{1}H NMR spectroscopy. The block copolymer self-assembly was achieved using two different methods, the non-selective-selective solvent dissolution method and the thin film hydration technique. The size of the nanocarriers was determined by DLS and their morphology was confirmed by FE SEM and TEM. The size of the micelles was smaller for the first method (28 to 172 nm) compared to the second method (150-170 nm) and was found to depend on the copolymer architecture and composition. Similar results were obtained by SEM and TEM.

Finally, the release profile of Sudan Red 7b from the copolymer micelles was studied. Dye loaded micelles were prepared using the first method and the release of the dye was monitored at 37°C to simulate the body temperature.

The results showed a maximum release of 90% after 5 days for the diblock copolymer micelles and a faster release for the triblock copolymers which was composition dependent (95% and 73% after only 2 days). In order to slow down even further the release of the dye, mixed diblock and triblock copolymer micelles were prepared. A mixture of PEG-*b*-PLLA and PLLA-*b*-PEG-*b*-PLLA can self-assemble into more complex nanostructures which exhibited a much slower release of the drug molecules (58% after 14 days).

The obtained results are very promising for the use of these nanocarriers in sustained ocular drug delivery.

Future work will explore the release mechanism of the dye from the nanocarriers as well as their use in ocular drug delivery.

REFERENCES

[1] A. Mandal, R. Bisht, I. D. Rupenthal, and A. K. Mitra, "Polymeric micelles for ocular drug delivery: From structural frameworks to recent preclinical studies," *J. Control. Release*, vol. 248, pp. 96–116, 2017, doi: 10.1016/j.jconrel.2017.01.012.

[2] C. Zhang, L. Liao, and S. Gong, "Microwave-assisted synthesis of PLLA-PEG-PLLA triblock copolymers," *Macromol. Rapid Commun.*, vol. 28, no. 4, pp. 422–427, 2007, doi: 10.1002/marc.200600709.

[3] Y. H. A. Hussein and M. Youssry, "Polymeric micelles of biodegradable diblock copolymers: Enhanced encapsulation of hydrophobic drugs," *Materials*. 2018, doi: 10.3390/ma11050688.

[4] K. K. Jain, "Drug delivery systems - An overview," *Methods Mol. Biol.*, vol. 437, pp. 1–50, 2008, doi: 10.1007/978-1-59745-210-6_1.

[5] S. S. Venkatraman, P. Jie, F. Min, B. Y. C. Freddy, and G. Leong-Huat, "Micelle-like nanoparticles of PLA-PEG-PLA triblock copolymer as chemotherapeutic carrier," *Int. J. Pharm.*, vol. 298, no. 1, pp. 219–232, 2005, doi: 10.1016/j.ijpharm.2005.03.023.

[6] C. H. Tsai, P. Y. Wang, I. C. Lin, H. Huang, G. S. Liu, and C. L. Tseng, "Ocular drug delivery: Role of degradable polymeric nanocarriers for ophthalmic application," *International Journal of Molecular Sciences*, vol. 19, no. 9. 2018, doi: 10.3390/ijms19092830.

[7] W. Gao, J. M. Chan, and O. C. Farokhzad, "PH-responsive nanoparticles for drug delivery," *Molecular Pharmaceutics*, vol. 7, no. 6. American Chemical Society, pp. 1913–1920, Dec. 06, 2010, doi: 10.1021/mp100253e.

[8] L. Zhang *et al.*, "Self-assembled lipid-polymer hybrid nanoparticles: A robust drug delivery platform," *ACS Nano*, vol. 2, no. 8, pp. 1696–1702, Aug. 2008, doi: 10.1021/nn800275r.

[9] S. Liu, L. Jones, and F. X. Gu, "Nanomaterials for Ocular Drug Delivery," *Macromol. Biosci.*, vol. 12, no. 5, pp. 608–620, May 2012, doi: 10.1002/mabi.201100419.

[10] E. M. del Amo, *Ocular and systemic pharmacokinetic models for drug discovery and development*. 2015.

[11] P. R. Karn, H. Do Kim, H. Kang, B. K. Sun, S. E. Jin, and S. J. Hwang, "Supercritical fluid-mediated liposomes containing cyclosporin A for the treatment of dry eye syndrome in a rabbit model: Comparative study with the conventional cyclosporin A emulsion," *Int. J. Nanomedicine*, 2014, doi: 10.2147/IJN.S65601.

[12] B. D. Ulery, L. S. Nair, and C. T. Laurencin, "Biomedical applications of biodegradable polymers," *Journal of Polymer Science, Part B: Polymer Physics*. 2011, doi: 10.1002/polb.22259.

[13] H. K. Makadia and S. J. Siegel, "Poly Lactic-co-Glycolic Acid (PLGA) as biodegradable controlled drug delivery carrier," *Polymers (Basel).*, 2011, doi: 10.3390/polym3031377.

[14] M. S. Muthu, "Nanoparticles based on PLGA and its co-polymer: An overview," *Asian J. Pharm.*, vol. 3, no. 4, pp. 266–273, 2009, doi: 10.4103/0973-8398.59948.

[15] C. Cañadas *et al.*, "In vitro, ex vivo and in vivo characterization of PLGA nanoparticles loading pranoprofen for ocular administration," *Int. J. Pharm.*, 2016, doi: 10.1016/j.ijpharm.2016.07.055.

[16] K. Nagpal, S. K. Singh, and D. N. Mishra, "Chitosan nanoparticles: A promising system in novel drug delivery," *Chemical and Pharmaceutical Bulletin*. 2010, doi: 10.1248/cpb.58.1423.

[17] R. C. Nagarwal, P. N. Singh, S. Kant, P. Maiti, and J. K. Pandit, "Chitosan nanoparticles of 5-fluorouracil for ophthalmic delivery: Characterization, in-vitro and in-vivo study," *Chem. Pharm. Bull.*, 2011, doi: 10.1248/cpb.59.272.

[18] N. C. Silva, S. Silva, B. Sarmento, and M. Pintado, "Chitosan nanoparticles for daptomycin delivery in ocular treatment of bacterial endophthalmitis," *Drug Deliv.*, 2015, doi: 10.3109/10717544.2013.858195.

[19] S. Biswas, O. S. Vaze, S. Movassaghian, and V. P. Torchilin, "Polymeric Micelles for the Delivery of Poorly Soluble Drugs," *Drug Deliv. Strateg. Poorly Water-Soluble Drugs*, pp. 411–476, 2013, doi: 10.1002/9781118444726.ch14.

[20] D. A. Chiappetta and A. Sosnik, "Poly(ethylene oxide)-poly(propylene oxide) block copolymer micelles as drug delivery agents: Improved hydrosolubility, stability and bioavailability of drugs," *European Journal of Pharmaceutics and Biopharmaceutics*, vol. 66, no. 3. Elsevier, pp. 303–317, Jun. 01, 2007, doi:

10.1016/j.ejpb.2007.03.022.

[21] S. Fusco, A. Borzacchiello, and P. A. Netti, “Perspectives on: PEO-PPO-PEO Triblock Copolymers and their Biomedical Applications,” *J. Bioact. Compat. Polym.*, vol. 21, no. 2, pp. 149–164, Mar. 2006, doi: 10.1177/0883911506063207.

[22] I. G. Shin, S. Y. Kim, Y. M. Lee, C. S. Cho, and Y. K. Sung, “Methoxy poly(ethylene glycol)/ε-caprolactone amphiphilic block copolymeric micelle containing indomethacin. I. Preparation and characterization,” *J. Control. Release*, vol. 51, no. 1, pp. 1–11, Jan. 1998, doi: 10.1016/S0168-3659(97)00164-8.

[23] C. Allen, Y. Yu, D. Maysinger, and A. Eisenberg, “Polycaprolactone-b-poly(ethylene oxide) block copolymer micelles as a novel drug delivery vehicle for neurotrophic agents FK506 and L-685,818,” *Bioconjug. Chem.*, vol. 9, no. 5, pp. 564–572, Sep. 1998, doi: 10.1021/bc9702157.

[24] F. Chen, G. Yin, and X. Liao, “Preparation , characterization and in vitro release properties of morphine-loaded PLLA-PEG-PLLA microparticles via solution enhanced dispersion by supercritical fluids,” pp. 1693–1705, 2013, doi: 10.1007/s10856-013-4926-1.

[25] X. Deng, S. Zhou, X. Li, J. Zhao, and M. Yuan, “In vitro degradation and release profiles for poly-dl-lactide-poly(ethylene glycol) microspheres containing human serum albumin,” *J. Control. Release*, 2001, doi: 10.1016/S0168-3659(01)00210-3.

[26] H. Danafar, K. Rostamizadeh, S. Davaran, and M. Hamidi, “PLA-PEG-PLA copolymer-based polymersomes as nanocarriers for delivery of hydrophilic and hydrophobic drugs: Preparation and evaluation with atorvastatin and lisinopril,” *Drug Dev. Ind. Pharm.*, vol. 40, no. 10, pp. 1411–1420, 2014, doi: 10.3109/03639045.2013.828223.

[27] C. Mu *et al.*, “Solubilization of flurbiprofen into aptamer-modified PEG-PLA micelles for targeted delivery to brain-derived endothelial cells in vitro,” *J. Microencapsul.*, vol. 30, no. 7, pp. 701–708, 2013, doi: 10.3109/02652048.2013.778907.

[28] M. Imran, M. R. Shah, and Shafiullah, “Amphiphilic block copolymers–based micelles for drug delivery,” in *Design and Development of New Nanocarriers*, Elsevier Inc., 2018, pp. 365–400.

[29] W. Zhou, C. Li, Z. Wang, W. Zhang, and J. Liu, “Factors affecting the stability of drug-loaded polymeric micelles and strategies for improvement,” *J. Nanoparticle Res.*, vol. 18, no. 9, pp. 1–18, 2016, doi: 10.1007/s11051-016-3583-y.

[30] Y. Mai and A. Eisenberg, “Self-assembly of block copolymers,” *Chem. Soc. Rev.*, vol. 41, no. 18, pp. 5969–5985, Aug. 2012, doi: 10.1039/c2cs35115c.

[31] S. C. Owen, D. P. Y. Chan, and M. S. Shoichet, “Polymeric micelle stability,” *Nano Today*, vol. 7, pp. 53–65, 2012, doi: 10.1016/j.nantod.2012.01.002.

[32] K. E. Uhrich, S. M. Cannizzaro, R. S. Langer, and K. M. Shakesheff, “Polymeric Systems for Controlled Drug Release,” *Chem. Rev.*, vol. 99, no. 11, pp. 3181–3198, 1999, doi: 10.1021/cr940351u.

[33] R. Z. Xiao, Z. W. Zeng, G. L. Zhou, J. J. Wang, F. Z. Li, and A. M. Wang, “Recent advances in PEG-PLA block copolymer nanoparticles,” *Int. J. Nanomedicine*, vol. 5, no. 1, pp. 1057–1065, 2010, doi: 10.2147/IJN.S14912.

[34] T. Niwa, H. Takeuchi, T. Hino, N. Kunou, and Y. Kawashima, “Preparations of biodegradable nanospheres of water-soluble and insoluble drugs with D,L-lactide/glycolide copolymer by a novel spontaneous emulsification solvent diffusion method, and the drug release behavior,” *J. Control. Release*, 1993, doi: 10.1016/0168-3659(93)90097-O.

[35] Z. L. Yang, R. L. Xin, W. Y. Ke, and Y. Liu, “Amphotericin B-loaded poly(ethylene glycol)-poly(lactide) micelles: Preparation, freeze-drying, and in vitro release,” *J. Biomed. Mater. Res. - Part A*, 2008, doi: 10.1002/jbm.a.31504.

[36] Y. Luo, X. Yao, J. Yuan, T. Ding, and Q. Gao, “Preparation and drug controlled-release of polyion complex micelles as drug delivery systems,” *Colloids Surfaces B Biointerfaces*, vol. 68, no. 2, pp. 218–224, Feb. 2009, doi: 10.1016/j.colsurfb.2008.10.014.

[37] Y. Wang, P. Li, T. T. D. Tran, J. Zhang, and L. Kong, “Manufacturing techniques and surface engineering of polymer based nanoparticles for targeted drug delivery to cancer,” *Nanomaterials*, vol. 6, no. 2, 2016, doi: 10.3390/nano6020026.

[38] A. D. Jenkins, R. F. T. Stepto, P. Kratochvíl, and U. W. Suter, “Glossary of basic terms in polymer science (IUPAC Recommendations 1996),” *Pure Appl. Chem.*, vol. 68, no. 12, pp. 2287–2311, Jan. 1996, doi:

10.1351/pac199668122287.

[39] S. Metkar, V. Sathe, I. Rahman, B. Idage, and S. Idage, “Ring opening polymerization of lactide: kinetics and modeling,” *Chem. Eng. Commun.*, vol. 206, no. 9, pp. 1159–1167, 2019, doi: 10.1080/00986445.2018.1550395.

[40] O. Nuyken and S. D. Pask, “Ring-opening polymerization-An introductory review,” *Polymers (Basel).*, vol. 5, no. 2, pp. 361–403, 2013, doi: 10.3390/polym5020361.

[41] C. Vauthier and K. Bouchemal, “Methods for the Preparation and Manufacture of Polymeric Nanoparticles,” *Pharmaceutical Research*, vol. 26, no. 5. Springer New York, pp. 1025–1058, Dec. 24, 2009, doi: 10.1007/s11095-008-9800-3.

[42] C. I. C. Crucho and M. T. Barros, “Polymeric nanoparticles: A study on the preparation variables and characterization methods,” *Materials Science and Engineering C*, vol. 80. Elsevier Ltd, pp. 771–784, Nov. 01, 2017, doi: 10.1016/j.msec.2017.06.004.

[43] C. Ma, P. Pan, G. Shan, Y. Bao, M. Fujita, and M. Maeda, “Core-Shell structure, biodegradation, and drug release behavior of poly(lactic acid)/poly(ethylene glycol) block copolymer micelles tuned by macromolecular stereostructure,” *Langmuir*, vol. 31, no. 4, pp. 1527–1536, 2015, doi: 10.1021/la503869d.

[44] K. K. Gill, A. Kaddoumi, and S. Nazzal, “PEG-lipid micelles as drug carriers: Physiochemical attributes, formulation principles and biological implication,” *J. Drug Target.*, vol. 23, no. 3, pp. 222–231, Apr. 2015, doi: 10.3109/1061186X.2014.997735.

[45] L. Yang, A. El Ghzaoui, and S. Li, “In vitro degradation behavior of poly(lactide)-poly(ethylene glycol) block copolymer micelles in aqueous solution,” *Int. J. Pharm.*, vol. 400, no. 1–2, pp. 96–103, Nov. 2010, doi: 10.1016/j.ijpharm.2010.08.037.